Journal of Cerebral Blood Flow & Metabolism (2014) 34, 332–338

www.jcbfm.com

ORIGINAL ARTICLE

Lesion development and reperfusion benefit in relation to vascular occlusion patterns after embolic stroke in rats

Mark JRJ Bouts[1,2], Ivo ACW Tiebosch[1], Annette van der Toorn[1], Jeroen Hendrikse[3] and Rick M Dijkhuizen[1]

Vascular occlusion sites largely determine the pattern of cerebral tissue damage and likelihood of subsequent reperfusion after acute ischemic stroke. We aimed to elucidate relationships between flow obstruction in segments of the internal carotid artery (ICA) and middle cerebral artery (MCA), and (1) profiles of acute ischemic lesions and (2) probability of subsequent beneficial reperfusion. Embolic stroke was induced by unilateral intracarotid blood clot injection in normotensive ($n = 53$) or spontaneously hypertensive ($n = 20$) rats, followed within 2 hours by magnetic resonance (MR) angiography (MRA), diffusion- (DWI) and perfusion-weighted magnetic resonance imaging (MRI) (PWI). In a subset of animals ($n = 9$), MRI was repeated after 24 and 168 hours to determine the predictive value of the occlusion pattern on benefit of reperfusion. The extent of cerebral perfusion and diffusion abnormality was related to the pattern of flow obstruction in ICA and MCA segments. Hypertensive animals displayed significantly larger cortical perfusion lesions. Acute perfusion-diffusion lesion mismatches were detected in all animals that subsequently benefitted from reperfusion. Yet, the presence of an angiography-diffusion mismatch was more specific in predicting reperfusion benefit. Combination of DWI, PWI, and MRA exclusively informs on the impact of arterial occlusion profiles after acute ischemic stroke, which may improve prognostication and subsequent treatment decisions.

Journal of Cerebral Blood Flow & Metabolism (2014) **34,** 332–338; doi:10.1038/jcbfm.2013.202; published online 4 December 2013

Keywords: diffusion-weighted imaging; ischemic stroke; magnetic resonance angiography perfusion imaging; prediction

INTRODUCTION

Acute magnetic resonance imaging (MRI) significantly contributes to early diagnosis and subsequent treatment planning in patients suffering from acute ischemic stroke.[1] Tissue amenable for thrombolytic treatment may be identified from a volumetric mismatch between brain areas with reduced tissue diffusion and perfusion, i.e., the perfusion-diffusion mismatch, measured from diffusion- (DWI) and perfusion-weighted imaging (PWI).[2] However, the perfusion-diffusion mismatch may also overestimate the area of tissue at risk of infarction or exclude potentially salvageable tissue.[3]

A major factor in the development of an ischemic lesion is the location and extent of vessel occlusion, which may be identified by angiography. Recently, the concept of a magnetic resonance (MR) angiography (MRA)-diffusion mismatch has been introduced, which indicates the presence of intracranial vessel occlusion or stenosis detected with MRA and a relatively small lesion detected with DWI.[4] The angiography-diffusion mismatch represents tissue without diffusion abnormality within the vascular territory of the occluded artery, i.e., tissue at risk. However, the concept of the angiography-diffusion mismatch has been disputed as it may disregard possible compensatory mechanisms of collateral flow from other feeding arteries, and as such may overestimate tissue at risk of infarction.[3,5,6]

The aims of the current study were to determine the relationship between ischemic lesion patterns and vascular occlusion profiles, and to compare the efficacy of the perfusion-diffusion and angiography-diffusion mismatch paradigms in predicting benefit from subsequent reperfusion. Our experimental study in which acute embolic stroke was induced in normotensive rats, and in spontaneously hypertensive rats (which have impaired collateral flow[7]), allowed us to (1) correlate the development of acute ischemic lesions, as measured with DWI and PWI, with the pattern of flow obstruction in segments of the Circle of Willis, as measured with MRA, and (2) establish the sensitivity and specificity of the angiography-diffusion and perfusion-diffusion mismatch concepts to predict tissue salvageability on reperfusion.

MATERIALS AND METHODS

Experimental Stroke Model

This study involved *post hoc* analysis of imaging data from animals that were used in two randomized treatment studies[8] (Tiebosch, Bouts, Dijkhuizen, unpublished data, 2013). The objectives, angiography data, and analyses in the present study are original and were not part of the earlier treatment papers.

Animal procedures were conducted according to the guidelines of the European Communities Council Directive and approved by the Ethical Committee on Animal Experiments of the University Medical Center Utrecht and Utrecht University. Rats were intubated and mechanically ventilated with 2% isoflurane in air to O_2 (2:1). All animals received a 5 mg/kg injection of gentamicin as antibiotic, and a 2.5 mL injection with glucose (2.5%) in saline to prevent dehydration. Body temperature was maintained at $37.5 \pm 0.5\ ^{\circ}C$ with a temperature-controlled heating pad. Thromboembolic stroke was induced as described earlier.[8,9] In brief, the right carotid

[1]Biomedical MR Imaging and Spectroscopy Group, Image Sciences Institute, University Medical Center Utrecht, Utrecht, The Netherlands; [2]Athinoula A. Martinos Center for Biomedical Imaging, Massachusetts General Hospital, Harvard Medical School, Charlestown, Massachusetts, USA and [3]Department of Radiology, University Medical Center Utrecht, Utrecht, The Netherlands. Correspondence: Dr RM Dijkhuizen, Biomedical MR Imaging and Spectroscopy Group, Image Sciences Institute, Heidelberglaan 100, Utrecht 3584 CX, The Netherlands. E-mail: r.m.dijkhuizen@umcutrecht.nl

The research leading to these results was funded by the Netherlands Heart Foundation (2005B156), and the European Union's Seventh Framework Programme (FP7/2007-2013) under grant agreements no. 201024 and no. 202213 (European Stroke Network).
Received 16 July 2013; revised 8 October 2013; accepted 25 October 2013; published online 4 December 2013

artery was exposed by a ventral incision in the neck. A modified catheter was advanced into the internal carotid artery (ICA), until the tip was positioned just proximal to the middle cerebral artery (MCA). A homologous blood clot was injected slowly followed by careful removal of the catheter. The wound was closed and animals were prepared for MRI (see below).

Postoperative care included additional subcutaneous injections with 0.03 mg/kg buprenorphine (Temgesic®, Schering-Plough, Houten, The Netherlands) and 2.5% glucose in saline (2.5 mL) for compensation of fluid loss. The animals were daily weighed, and excessive weight loss during the first 3 days after stroke was partly compensated with daily Ringer's lactate administration (0 to 10 mL, depending on the amount of loss of body weight).

Right-sided unilateral stroke was induced in normotensive male Wistar rats (normotensive group; $n = 82$, 341 ± 39 g) (Harlan, Venray, The Netherlands)[8] or spontaneously hypertensive Wistar-Kyoto rats (hypertensive group; $n = 24$, 303 ± 21 g) (Charles River, Sulzfeld, Germany) (Tiebosch, Bouts, Dijkhuizen, unpublished data, 2013), by intracarotid injection of a homologous blood clot—obtained 24 hours before stroke induction—near the bifurcation of the ICA and MCA.

Animals were included for this study if MRA, DWI, and PWI (see below) were acquired within 2 hours after stroke onset, and if acute tissue and perfusion lesion volumes were larger than 1 mm^3. From a subset of rats (seven normotensive and two hypertensive rats) that underwent follow-up MRI, we included animals that showed effective reperfusion at 24 hours after stroke, defined as a perfusion lesion volume reduction of $>30\%$ compared with the acute perfusion lesion volume,[4] to assess reperfusion benefit.

Magnetic Resonance Imaging and Angiography

The MRI was conducted on a 4.7-T scanner (Agilent, Palo Alto, CA, USA) immediately after stroke induction, and repeated at 24 and 168 hours after stroke onset in a subset of animals. Animals were mechanically ventilated with 2% isoflurane in air to O_2 (2:1).

For all MRI acquisitions, field-of-view was set to 32×32 mm^2, with 1 mm slice thickness. The MRI protocol consisted of multiple spin-echo T_2-weighted images (repetition time 3,600 ms; echo time 12 to 144 ms; data matrix size $256 \times 128 \times 19$) for reconstruction of quantitative T_2 maps by nonlinear least square fitting. Maps of the apparent diffusion coefficient (ADC) were calculated from diffusion-weighted 8-shot echo planar imaging (repetition time 3,500 ms; echo time 38.5 ms; *b* values 0 and 1,428 s/mm^2; 6 diffusion-weighted direction; data matrix size $128 \times 128 \times 19$). Dynamic susceptibility contrast-enhanced MRI was executed with gradient echo planar imaging (repetition time 330 ms; echo time 25 ms; data matrix size $64 \times 64 \times 5$) in combination with an intravenous bolus injection of 0.35 mmol/kg gadobutrol (Gadovist, Schering, The Netherlands). Maps of the cerebral blood flow, cerebral blood volume, mean transit time (MTT), and bolus peak time (T_{max}) were subsequently acquired by circular deconvolution of the tissue concentration curves with an arterial reference curve obtained from the contralateral hemisphere.[10] Magnetic resonance angiography was executed with a flow-compensated 3D time-of-flight sequence (gradient echo; repetition time 15 ms; echo time 2.66 ms; field-of-view $32 \times 32 \times 32$ mm^3; data matrix size $128 \times 128 \times 128$).

Image Processing and Analysis

Voxels with abnormal ADC (i.e., tissue lesion) or MTT (i.e., perfusion lesion) were identified from differences of >2 standard deviations from mean contralateral tissue values in four consecutive slices.[10] Perfusion-diffusion mismatch volume was calculated from the difference between the total volumes of ADC and MTT abnormality. The presence of a significant perfusion-diffusion mismatch was confirmed when the MTT-based perfusion lesion volume was 20% larger than the ADC-based tissue lesion volume.[4]

Sites of flow obstruction were assessed on MR angiograms by an experienced observer (IT). Vessel segments were scored for the presence ('0') or the absence of flow ('1'), to warrant unambiguous identification of complete occlusion.[4,5] Subsequently, arterial occlusion patterns were categorized in eight different 'Occlusion Severity' grades according to occlusions of the ICA and/or the proximal (M1) or distal (M2) branches of the MCA (Table 1).

Angiography-diffusion mismatch was defined as the presence of ICA and/or MCA occlusion in combination with an ADC-based tissue lesion volume of <24 mm^3 (proportional to the defined 25 mL in $\sim 1{,}030\times$ larger human brain[4]). In addition, we defined a combinatory angiography-perfusion-diffusion mismatch characterized by a perfusion-diffusion mismatch in the presence of ICA and/or MCA occlusion.

Table 1. Vessel occlusion patterns and their incidences in normotensive and hypertensive rats after intracarotid embolic clot injection

Occlusion pattern				*% Age incidence*	
Grade	*ICA*	*MCA.M1*	*MCA.M2*	*Normotensive group*	*Hypertensive group*
I	0	0	0	36	45
II	0	0	1	15	10
III	1	0	0	17	20
IV	0	1	0	0	0
V	0	1	1	4	5
VI	1	1	0	2	0
VII	1	0	1	9	0
VIII	1	1	1	17	20

ICA, internal carotid artery; MCA.M1, M1 branch of the middle cerebral artery; MCA.M2, M2 branch of the middle cerebral artery. Occlusion scores: 0: non-occluded; 1: occluded. Total numbers of animals were 53 for the normotensive group and 20 for the hypertensive group. Twenty-nine normotensive and four hypertensive animals were excluded because of late onset of imaging, too small lesion size, or mortality.

Benefit of reperfusion was defined as the absence of lesion growth beyond 10% of the acute ADC-based tissue lesion volume, as measured from the follow-up T_2 lesion volume at poststroke day 7 (calculated as the ipsilateral tissue volume with T_2 values above 2 standard deviations from mean contralateral tissue values[10]).

To test the predictive value of the two mismatch models, animals were divided into four groups for each mismatch model: those with a mismatch that subsequently benefitted from reperfusion (true positive, TP), those with a mismatch that subsequently did not benefit from reperfusion (false positive, FP), those without a mismatch that benefitted from reperfusion (false negative, FN), and those without a mismatch that did not benefit from reperfusion (true negative, TN). Sensitivity (TP/(TP + FN)), specificity (TN/(FP + TN)), and odds ratio (OR) of benefit of reperfusion were calculated for animals with an acute perfusion-diffusion mismatch or angiography-diffusion mismatch.

Statistics

Fisher's exact test was applied to determine differences in distribution of the vessel occlusion grades. Lesion volumes were compared using a Kruskal–Wallis test, with *post hoc* Mann–Whitney testing with false discovery rate correction for multiple comparisons. Linear mixed effects regression was used for correlating lesion volumes with the corresponding vessel occlusion grades. Odds ratios were calculated from 2×2 tables with Haldane's correction for sparse data.

RESULTS

A total of 73 rats (53 normotensive and 20 hypertensive animals) fulfilled the inclusion criteria, i.e., MRA and MRI within 2 hours, and acute ADC- and MTT-based lesion volumes larger than 1 mm^3.

Figure 1 shows examples of MR angiograms of rats' Circle of Willis with the absence of flow in the ipsilateral ICA, proximal (M1), and/or distal (M2) segments of the MCA acutely after intracarotid blood clot injection. In all, 36% and 45% of the normotensive and hypertensive animals, respectively, did not display absolute vessel occlusion of the ipsilateral ICA or MCA. The MRA data from all other animals showed unequivocal occlusions, with largest incidence of ICA occlusion with (occlusion grade VIII) or without (occlusion grade III) complete occlusion of the MCA (Table 1).

Figure 1 also shows the acute tissue and perfusion lesion on ADC and MTT maps, respectively, corresponding to the vessel occlusion grades as shown in the MR angiograms. The topographic distribution of acute tissue and perfusion lesions

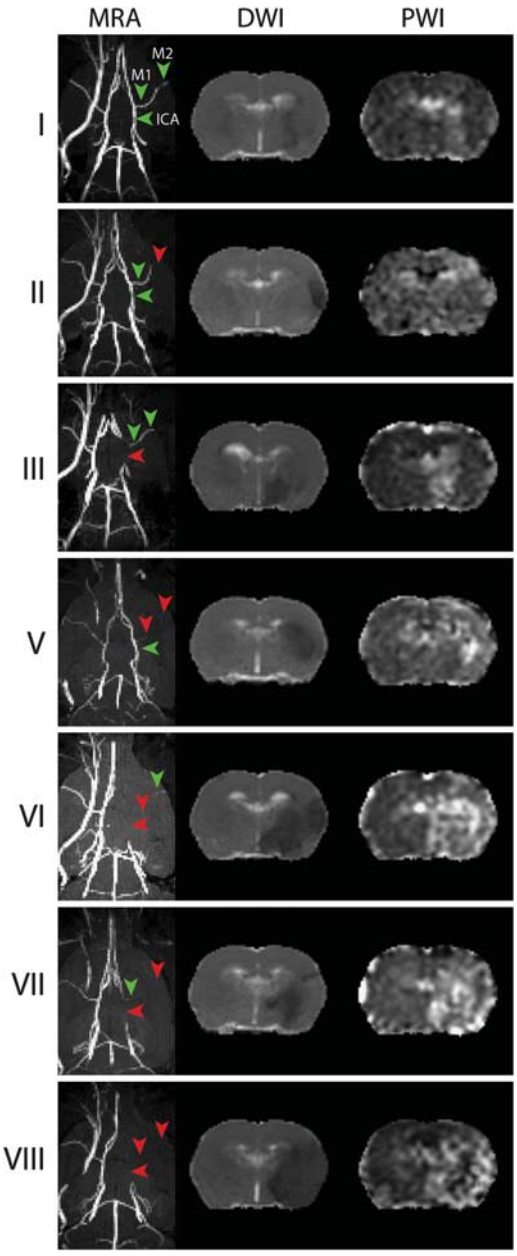

Figure 1. Examples of magnetic resonance angiography (MRA), diffusion-weighted imaging (DWI) and perfusion-weighted imaging (PWI) scans for the different levels of 'Occlusion Severity' grades (I to VIII) in normotensive rats. MR angiograms (MRAs) (transversal maximum intensity projection) reveal flow obstructions in the right internal carotid artery (ICA), MCA.M1, and MCA.M2 (red arrowheads) (green arrowheads show patent right ICA, MCA.M1, and MCA.M2). Apparent diffusion coefficient (ADC) (DWI) and mean transit time (MTT) (PWI) brain maps (coronal slice) show corresponding right-sided ischemic lesions with reduced ADC and prolonged MTT in the MCA territory. MCA, middle cerebral artery.

depended on the vessel occlusion pattern. Figure 2 shows lesion incidence maps for the different occlusion grades. Occlusion grades I and III, with incomplete occlusion of the MCA, resulted in mainly subcortical lesions in normotensive animals, with additional cortical involvement in hypertensive animals. This was also observed for single occlusion of the ICA (grade III). Occlusion grade II, which involved occlusion of the distal (M2) part of the MCA only, primarily affected cortical tissue. Occlusion of the proximal (M1) part of the MCA (grades V, VI, VII, and VIII) resulted in lesions in subcortical and cortical areas, with largest lesion volumes when flow was obstructed in ICA, MCA.M1, and MCA.M2 (occlusion grade VIII).

Quantified acute tissue and perfusion lesion volumes are shown in Figure 3, which showed that flow obstruction involving ICA and both branches of the MCA, resulted in significantly larger acute tissue lesions as compared with occlusion patterns in which flow in the proximal part of the MCA (MCA.M1) was preserved ($P<0.05$). However, the area of hypoperfusion was not significantly different between occlusion grades.

Hypertensive animals developed larger perfusion lesion volumes than normotensive animals, with largest difference for grade II and VIII occlusions ($P<0.05$). Acute tissue diffusion lesion volumes were also larger in hypertensive animals as compared with normotensive animals (61.8 ± 55.5 versus $20.9\pm17.9\,mm^3$), but statistically this was not significantly different.

Significant difference between the individual acute perfusion and tissue lesion volumes, i.e., perfusion-diffusion mismatch, was observed for normotensive rats in occlusion grades II, III, and VII, and only for hypertensive rats in occlusion grade I ($P<0.05$).

In the subset of rats that underwent follow-up MRI, reperfusion—i.e., $>30\%$ reduction in perfusion lesion volume—was observed in seven normotensive rats and two hypertensive rats. Follow-up T_2 lesion volumes at poststroke day 7 were significantly smaller than acute perfusion lesion volumes, and similar in size as acute diffusion lesions (see Figure 4 and Table 2). Ultimate lesion volume in reperfused hypertensive rats was larger than in reperfused normotensive rats (89.8 ± 29.9 versus $18.1\pm18.1\,mm^3$). Benefit from reperfusion was observed in all seven normotensive animals, but not in hypertensive animals. Perfusion-diffusion mismatch was detected in all nine animals, whereas an angiography-diffusion mismatch was observed in 44% of the animals. All animals with an angiography-diffusion mismatch also displayed a perfusion-diffusion mismatch. Benefit from reperfusion occurred in seven out of nine animals with a perfusion-diffusion mismatch (OR = 2.6), and four out of four animals with an angiography-diffusion mismatch (OR = 3.8). Although the sensitivity to detect reperfusion benefit was lower than that of the perfusion-diffusion mismatch (0.56 versus 0.89), the angiography-diffusion mismatch showed higher specificity (0.75 versus 0.25).

Combinatory angiography-perfusion-diffusion mismatch was detected in 67% of the animals of which six out of six with reperfusion benefit (OR = 10.5). Compared with the angiography-diffusion mismatch, sensitivity was increased (0.78 versus 0.56) with similar specificity (0.75).

DISCUSSION

In this study, we characterized the pattern of acute tissue and perfusion lesions in relation to the site of arterial flow obstruction after embolic stroke in rats, and assessed the potential of these profiles to predict benefit from reperfusion. We found that partial or complete occlusion of the ICA with incomplete flow obstruction in the proximal segment of the MCA (M1) resulted in predominantly subcortical lesions. Occlusions of the distal (M2) segment of the MCA resulted in primarily cortical injury. Large cortical and subcortical lesions were found when flow was lost in ICA and MCA segments. Lesion volumes were increased in hypertensive animals, which were particularly associated with a larger area of cortical hypoperfusion. Furthermore, we found that an angiography-diffusion mismatch was more specific in predicting potential benefit from reperfusion than a perfusion-diffusion mismatch. However, in contrast to consistent presence of an acute perfusion-diffusion mismatch in animals that benefitted from reperfusion, not all animals with reperfusion-induced prevention

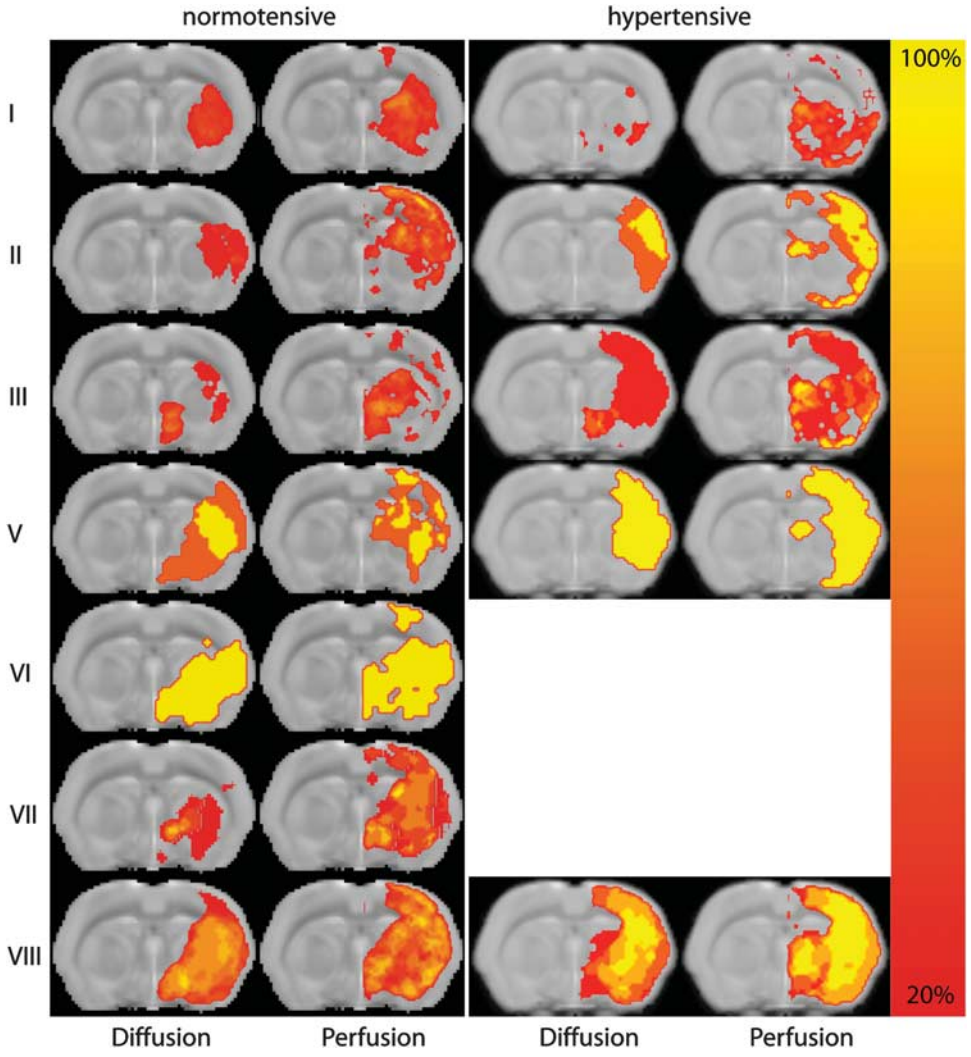

Figure 2. Incidence maps of tissue diffusion and perfusion abnormality in normotensive and hypertensive rats with different arterial occlusion patterns (grade IV was not present in any of the animals). Maps of lesion incidence (% of sample size) are overlaid on a coronal slice from a T_2-weighted anatomic rat brain template.

of lesion enlargement displayed an angiography-diffusion mismatch acutely after stroke.

In this study, we assessed the presence or absence of vascular flow in three segments of the ICA and MCA, distinguishing eight occlusion severity grades. Smallest volumes of acute abnormality on DWI were noted when partial flow was present in the ipsilateral ICA and MCA, whereas larger lesion volumes were observed for higher severity grades with complete vascular occlusions. This in line with previous studies that reported large infarct lesions in tandem occlusions of the ICA and the MCA, or proximal occlusions of the MCA, both in rats[11] and in patients.[12–14]

The area of perfusion abnormality differed less between occlusion grades, and significant perfusion-diffusion mismatch volumes were observed in ICA- and MCA.M2-occluded normotensive rats in which flow in MCA.M1 was partially preserved. This can be explained by the availability of alternative vascular routes that can compensate for the loss of flow from the main territorial artery. This compensatory flow may originate from other large vessels of the Circle of Willis, as well as leptomeningeal or extracranial arteries.[11,13,15,16] Occlusions of MCA.M1 were associated with relatively large lesions. Lenticulostriate arteries that originate from the proximal segment of the MCA form important perforating end connections to the basal ganglia and internal capsule, which receive little or no collateral blood flow.[17] Consequently, occlusion of the proximal segment of the MCA is typically performed to induce large, reproducible lesions in experimental stroke models,[11,15,18] and has been considered as a trade-off point for good outcome in clinical stroke patients.[14,19]

Rats with chronic hypertension developed larger acute and follow-up ischemic lesion volumes than those with normal blood pressure, in agreement with previous studies.[20,21] Chronic hypertension as a comorbidity may affect small arterial and arteriolar integrity via vascular hypertrophy, endothelial dysregulation, and atherosclerosis. These vascular alterations can significantly increase sensitivity to flow reductions and may also affect compensatory flow capabilities.[11,21,22] This can explain the lower incidence of perfusion-diffusion mismatches in hypertensive rats (it was only observed in animals with incomplete flow obstruction in all ICA and MCA segments). Furthermore, occlusion of the distal part of the MCA resulted in larger perfusion and tissue lesions in cortical tissue, suggestive of deficient recruitment of cortical arterial collaterals from leptomeningeal anastomoses and distal collaterals from the Circle of Willis in these animals.[7] However, larger lesions in spontaneously hypertensive rat strains may also be explained by higher tissue vulnerability linked to specific genetic factors.[20,23]

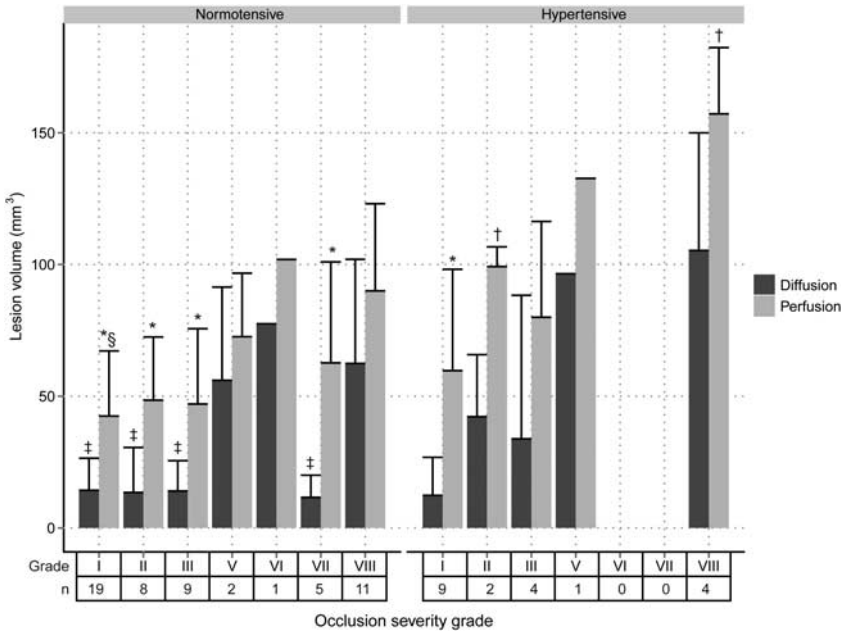

Figure 3. Volume (mean + s.d.) of perfusion and diffusion abnormality in normotensive and hypertensive animals with different occlusion severity grades (*n*: number of animals). $^{*}P<0.05$ versus diffusion lesion volume; $^{\dagger}P<0.05$ versus normotensive; $^{\ddagger}P<0.05$ versus grade VIII diffusion lesion volume; $^{\S}P<0.05$ versus grade VIII perfusion lesion volume.

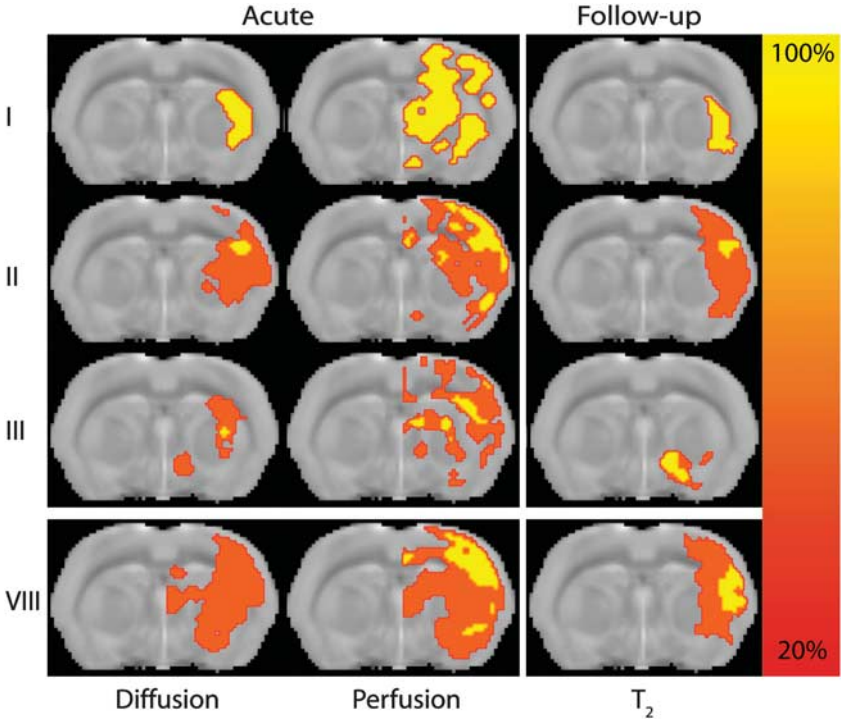

Figure 4. Incidence maps of acute tissue diffusion and perfusion abnormality, as well as follow-up T_2 abnormality in normotensive rats with different arterial occlusion patterns (grades IV, V, VI, and VII were not present in this subset of animals). Maps of lesion incidence (% of sample size) are overlaid on a coronal slice from a T_2-weighted anatomic rat brain template.

The angiography-diffusion mismatch, defined in acute stroke patients by a relatively small lesion on DWI in combination with MRA-based evidence of an intracranial stenosis or occlusion, has been proposed as an alternative means to identify patients that may benefit from reperfusion.[4] Our study in a rat embolic stroke model shows that animals with an angiography-diffusion mismatch showed no further lesion growth, with increased prediction specificity as compared with the perfusion-diffusion mismatch. Yet, some animals without an angiography-diffusion mismatch, but with a perfusion-diffusion mismatch, also displayed a therapeutic effect of reperfusion. Benefit from reperfusion is not only dependent on the site and extent of vascular occlusion,[24] but

Table 2. Characteristics of reperfused animals with acute perfusion-diffusion, angiography-diffusion and/or angiography-perfusion-diffusion mismatch

	PDM	*ADM*	*APDM*
Mismatch incidence	9/9	4/9	6/9
Acute perfusion lesion (mm^3)	67.7 ± 23.0	56.0 ± 20.2	62.1 ± 26.1
Acute diffusion lesion (mm^3)	24.4 ± 22.4	7.1 ± 1.8	24.8 ± 24.2
Follow-up T_2 lesion (mm^3)	34.1 ± 36.8	22.9 ± 30.6	19.6 ± 19.3
Incidence of reperfusion benefit	7/9	4/4	6/6
OR (95% confidence interval)	2.6 (0.1–57.6)	3.8 (0.3–51.4)	10.5 (0.6–165.1)
Sensitivity	0.89	0.56	0.78
Specificity	0.25	0.75	0.75

ADM, angiography-diffusion mismatch; APDM, angiography-perfusion-diffusion mismatch; OR, odds ratio; PDM, perfusion-diffusion mismatch.

also depends on local microvascular patency[25] and capability to accommodate collateral flow to the affected area.[16] Collateral flow may not only prolong tissue salvageability,[3,19] it may also improve thrombolytic efficacy by providing additional delivery routes to the site of occlusion.[13] Despite the potential of the angiography-diffusion mismatch to aid in identifying tissue salvageability on reperfusion, it does not provide direct information on local perfusion or collateral flow.[3,26] Additionally, MRA (especially time-of-flight MRA) has decreased sensitivity to flow in more distal parts of the arterial tree, which may lead to inexact assessment of the degree of arterial obstruction.[6] Future studies that include methods that enable quantitative measurement of collateral flow could significantly contribute to better understanding of the perfusion-diffusion mismatch and improved assessment of tissue salvageability after stroke.

Some caution in interpretation of our findings on mismatch volumes may be warranted. Due to the retrospective nature of our study, relatively small and unmatched subset of animals were used in this part of the analysis, which may have influenced statistical power. Benefit of reperfusion was defined as the absence of lesion growth derived from T_2-based follow-up imaging compared with acute ADC-based tissue lesion volumes. Although these measures allow estimation of macroscopic lesion size, they do not provide explicit details on the histologic status of poststroke brain tissue. Furthermore, it remains to be determined how changes in lesion growth actually translate to alterations in functional outcome.

We applied, after proper adjustments for rat brain, thresholds that have been previously used in clinical studies to determine the tissue amenable for treatment.[1,4] However, cerebral ischemia is a dynamic process in which development of penumbral tissue depends on the severity and duration of ischemia. Single thresholds to dichotomize tissue in normal and lesioned tissue may oversimplify the underlying complex processes on an individual basis.[27]

The acute lesion on DWI is key in estimating both the perfusion-diffusion and the angiography-diffusion mismatch. The DWI lesion is assumed to identify the nonviable ('core') tissue. However, in line with earlier studies,[27] we observed partial recovery of the acute tissue lesion on DWI as compared with the actual irreversibly damaged tissue at follow-up (data not shown). Reversibility of diffusion abnormality is still a matter of debate,[27,28] but recent MR/PET studies revealed spatial variability of the metabolic rate of oxygen within acute DWI lesions with preserved viability in some parts.[3] Obviously, the use of complementary information on the severity of hypoperfusion, such as measured with PWI, contributes to improved assessment of ischemic tissue. Furthermore, voxel-based mappings, rather than regional analysis, may improve diagnostic accuracy by calculation of maps of statistical infarction probability,[10] collateral flow index,[29] or vascular territory.[30] The latter can be accomplished with MRA that would aid in outcome prediction based on the specific pattern of vascular occlusion.[13,31]

In conclusion, combined DWI, PWI, and MRA provide complementary insights into the cerebral and vascular status after acute ischemic stroke, which may advance outcome prediction and could improve treatment decision making.

DISCLOSURE/CONFLICT OF INTEREST

The authors declare no conflict of interest.

REFERENCES

1 Olivot JM, Marks MP. Magnetic resonance imaging in the evaluation of acute stroke. *Top Magn Reson Imag* 2008; **19**: 225–230.
2 Schlaug G, Benfield A, Baird AE, Siewert B, Lövblad KO, Parker RA *et al.* The ischemic penumbra operationally defined by diffusion and perfusion MRI. *Neurology* 1999; **53**: 1528–1537.
3 Sobesky J. Refining the mismatch concept in acute stroke: lessons learned from PET and MRI. *J Cereb Blood Flow Metab* 2012; **32**: 1416–1425.
4 Lansberg MG, Thijs VN, Bammer R, Olivot J-M, Marks MP, Wechsler LR *et al.* The MRA-DWI mismatch identifies patients with stroke who are likely to benefit from reperfusion. *Stroke* 2008; **39**: 2491–2496.
5 Kim SJ, Seok JM, Bang OY, Kim G-M, Kim KH, Jeon P *et al.* MR mismatch profiles in patients with intracranial atherosclerotic stroke: a comprehensive approach comparing stroke subtypes. *J Cereb Blood Flow Metab* 2009; **29**: 1138–1145.
6 De Silva DA, Brekenfeld C, Ebinger M, Christensen S, Barber PA, Butcher KS *et al.* The benefits of intravenous thrombolysis relate to the site of baseline arterial occlusion in the echoplanar imaging thrombolytic evaluation trial (EPITHET). *Stroke* 2010; **41**: 295–299.
7 Coyle P, Heistad DD. Blood flow through cerebral collateral vessels in hypertensive and normotensive rats. *Hypertension* 1986; **8**: II67.
8 Tiebosch IACW, Crielaard BJ, Bouts MJRJ, Zwartbol R, Salas-Perdomo A, Lammers T *et al.* Combined treatment with recombinant tissue plasminogen activator and dexamethasone phosphate-containing liposomes improves neurological outcome and restricts lesion progression after embolic stroke in rats. *J Neurochem* 2012; **123**: 65–74.
9 Zhang RL, Chopp M, Zhang ZG, Jiang Q, Ewing JR. A rat model of focal embolic cerebral ischemia. *Brain Res* 1997; **766**: 83–92.
10 Bouts MJRJ, Tiebosch IACW, van der Toorn A, Viergever MA, Wu O, Dijkhuizen RM. Early identification of potentially salvageable tissue with MRI-based predictive algorithms after experimental ischemic stroke. *J Cereb Blood Flow Metab* 2013; **33**: 1075–1082.
11 Overgaard K, Rasmussen RS, Johansen FF. The site of embolization related to infarct size, oedema and clinical outcome in a rat stroke model - further translational stroke research. *Exp Transl Stroke Med* 2010; **2**: 17.
12 Seitz RJ, Sondermann V, Wittsack H-J, Siebler M. Lesion patterns in successful and failed thrombolysis in middle cerebral artery stroke. *Neuroradiology* 2009; **51**: 865–871.
13 Cheng B, Golsari A, Fiehler J, Rosenkranz M, Gerloff C, Thomalla G. Dynamics of regional distribution of ischemic lesions in middle cerebral artery trunk occlusion relates to collateral circulation. *J Cereb Blood Flow Metab* 2011; **31**: 36–40.
14 Saarinen JT, Sillanpää N, Rusanen H, Hakomäki J, Huhtala H, Lähteelä A *et al.* The mid-M1 segment of the middle cerebral artery is a cutoff clot location for good outcome in intravenous thrombolysis. *Eur J Radiol* 2012; **19**: 1121–1127.

15 Bederson JB, Pitts LH, Tsuji M, Nishimura MC, Davis RL, Bartkowski H. Rat middle cerebral artery occlusion: evaluation of the model and development of a neurologic examination. *Stroke* 1986; **17**: 472–476.
16 Liebeskind DS. Collateral circulation. *Stroke* 2003; **34**: 2279–2284.
17 Marinkovic SV, Milisavljevic MM, Kovacevic MS, Stevic ZD. Perforating branches of the middle cerebral artery. Microanatomy and clinical significance of their intracerebral segments. *Stroke* 1985; **16**: 1022–1029.
18 Niiro M, Simon RP, Kadota K, Asakura T. Proximal branching patterns of middle cerebral artery (MCA) in rats and their influence on the infarct size produced by MCA occlusion. *J Neurosci Methods* 1996; **64**: 19–23.
19 Fiehler J, Knudsen K, Thomalla G, Goebell E, Rosenkranz M, Weiller C *et al.* Vascular occlusion sites determine differences in lesion growth from early apparent diffusion coefficient lesion to final infarct. *AJNR Am J Neuroradiol* 2005; **26**: 1056–1061.
20 Coyle P. Different susceptibilities to cerebral infarction in spontaneously hypertensive (SHR) and normotensive Sprague-Dawley rats. *Stroke* 1986; **17**: 520–525.
21 McCabe C, Gallagher L, Gsell W, Graham D, Dominiczak AF, MacRae IM. Differences in the evolution of the ischemic penumbra in stroke-prone spontaneously hypertensive and Wistar-Kyoto rats. *Stroke* 2009; **40**: 3864–3868.
22 Howells DW, Porritt MJ, Rewell SSJ, O'Collins V, Sena ES, van der Worp HB *et al.* Different strokes for different folks: the rich diversity of animal models of focal cerebral ischemia. *J Cereb Blood Flow Metab* 2010; **30**: 1412–1431.
23 Yasui M, Kawasaki K. Vulnerability of CA1 neurons in SHRSP hippocampal slices to ischemia, and its protection by $Ca^{2}+$ channel blockers. *Brain Res* 1994; **642**: 146–152.
24 Marks MP, Olivot J-M, Kemp S, Lansberg MG, Bammer R, Wechsler LR *et al.* Patients with acute stroke treated with intravenous tPA 3-6 hours after stroke onset: correlations between MR angiography findings and perfusion- and diffusion-weighted imaging in the DEFUSE study. *Radiology* 2008; **249**: 614–623.
25 Wang CX, Todd KG, Yang Y, Gordon T, Shuaib A. Patency of cerebral microvessels after focal embolic stroke in the rat. *J Cereb Blood Flow Metab* 2001; **21**: 413–421.
26 Schellinger PD, Köhrmann M. MRA/DWI mismatch: a novel concept or something one could get easier and cheaper? *Stroke* 2008; **39**: 2423–2424.
27 Kranz PG, Eastwood JD. Does diffusion-weighted imaging represent the ischemic core? An evidence-based systematic review. *AJNR Am J Neuroradiol* 2009; **30**: 1206–1212.
28 Campbell BCV, Purushotham A, Christensen S, Desmond PM, Nagakane Y, Parsons MW *et al.* The infarct core is well represented by the acute diffusion lesion: Sustained reversal is infrequent. *J Cereb Blood Flow Metab* 2012; **32**: 50–56.
29 Nicoli F, Lafaye de Micheaux P, Girard N. Perfusion-weighted imaging-derived collateral flow index is a predictor of MCA M1 recanalization after iv thrombolysis. *AJNR Am J Neuroradiol* 2013; **34**: 107–114.
30 Van Laar PJ, van der Grond J, Hendrikse J. Brain perfusion territory imaging: methods and clinical applications of selective arterial spin-labeling MR imaging. *Radiology* 2008; **246**: 354–364.
31 Menezes NM, Ay H, Wang Zhu M, Lopez CJ, Singhal AB, Karonen JO *et al.* The real estate factor quantifying the impact of infarct location on stroke severity. *Stroke* 2007; **38**: 194–197.